







## RESEARCH ARTICLE

# Spatiotemporal influences of climate and humans on muskox range dynamics over multiple millennia

Elisabetta Canteri<sup>1,2</sup>  | Stuart C. Brown<sup>1,3</sup>  | Niels Martin Schmidt<sup>4</sup>  |  
Rasmus Heller<sup>5</sup>  | David Nogués-Bravo<sup>2</sup>  | Damien A. Fordham<sup>1,2,6</sup> 

<sup>1</sup>The Environment Institute and School of Biological Sciences, University of Adelaide, Adelaide, South Australia, Australia

<sup>2</sup>Center for Macroecology, Evolution and Climate, Globe Institute, University of Copenhagen, Copenhagen, Denmark

<sup>3</sup>Section for Molecular Ecology and Evolution, Globe Institute, University of Copenhagen, Copenhagen, Denmark

<sup>4</sup>Department of Ecoscience and Arctic Research Centre, Aarhus University, Roskilde, Denmark

<sup>5</sup>Department of Biology, Section of Computational and RNA Biology, University of Copenhagen, Copenhagen, Denmark

<sup>6</sup>Center for Global Mountain Biodiversity, Globe Institute, University of Copenhagen, Copenhagen, Denmark

## Correspondence

Elisabetta Canteri and Damien A. Fordham, The Environment Institute and School of Biological Sciences, University of Adelaide, Adelaide, SA, 5005, Australia. Email: [elisabetta.canteri@adelaide.edu.au](mailto:elisabetta.canteri@adelaide.edu.au) and [damien.fordham@adelaide.edu.au](mailto:damien.fordham@adelaide.edu.au)

## Funding information

Australian Research Council, Grant/Award Number: DP180102392 and FT140101192; Danmarks Grundforskningsfond, Grant/Award Number: DNRF96

## Abstract

Processes leading to range contractions and population declines of Arctic megafauna during the late Pleistocene and early Holocene are uncertain, with intense debate on the roles of human hunting, climatic change, and their synergy. Obstacles to a resolution have included an overreliance on correlative rather than process-explicit approaches for inferring drivers of distributional and demographic change. Here, we disentangle the ecological mechanisms and threats that were integral in the decline and extinction of the muskox (*Ovibos moschatus*) in Eurasia and in its expansion in North America using process-explicit macroecological models. The approach integrates modern and fossil occurrence records, ancient DNA, spatiotemporal reconstructions of past climatic change, species-specific population ecology, and the growth and spread of anatomically modern humans. We show that accurately reconstructing inferences of past demographic changes for muskox over the last 21,000 years require high dispersal abilities, large maximum densities, and a small Allee effect. Analyses of validated process-explicit projections indicate that climatic change was the primary driver of muskox distribution shifts and demographic changes across its previously extensive (circumpolar) range, with populations responding negatively to rapid warming events. Regional analyses show that the range collapse and extinction of the muskox in Europe (~13,000 years ago) was likely caused by humans operating in synergy with climatic warming. In Canada and Greenland, climatic change and human activities probably combined to drive recent population sizes. The impact of past climatic change on the range and extinction dynamics of muskox during the Pleistocene–Holocene transition signals a vulnerability of this species to future increased warming. By better establishing the ecological processes that shaped the distribution of the muskox through space and time, we show that process-explicit macroecological models have important applications for the future conservation and management of this iconic species in a warming Arctic.

## KEYWORDS

Arctic, climate change, exploitation, extinction dynamics, mechanistic model, megafauna, range dynamics, spatially explicit population model

This is an open access article under the terms of the [Creative Commons Attribution-NonCommercial](https://creativecommons.org/licenses/by-nc/4.0/) License, which permits use, distribution and reproduction in any medium, provided the original work is properly cited and is not used for commercial purposes.

© 2022 The Authors. *Global Change Biology* published by John Wiley & Sons Ltd.

## 1 | INTRODUCTION

The Arctic is warming almost twice as fast as the rest of the world (Meredith et al., 2019; Screen & Simmonds, 2010), with mean annual temperatures forecast to increase by 3–12°C (above 2010 conditions) by the end of the 21st century (Lee et al., 2021). This warming is causing biodiversity change, which is disrupting the structure and function of ecological systems (Post et al., 2019). However, climatic conditions in the Arctic have rarely been stable, with temperatures fluctuating enormously during glacial–interglacial cycles (Dansgaard et al., 1993), resulting in large biotic change. These climate-driven biotic changes include declines in species distributions, population sizes and genetic diversity (Hansen et al., 2018; Lorenzen et al., 2011), regional and range-wide extinctions (Cooper et al., 2015; Stuart, 2015), shifts in community assembly (Wang et al., 2021), and ecosystem function (Zimov et al., 1995).

During the late Quaternary, vast areas of Earth's terrestrial ecosystems experienced warming events that are similar in magnitude and pace to conditions predicted for the end of the 21st century (Brown et al., 2020). Establishing biotic responses to these past warming events can improve projections of future biodiversity, through a better understanding of how different spatiotemporal scales of climatic change affect biodiversity (Fordham et al., 2020). However, this often requires integrating ecological and evolutionary models with fossil and molecular inferences of biotic change (Fordham et al., 2014; Nogues-Bravo et al., 2018). Although this has generally been done correlatively (Svenning et al., 2011), process-explicit models are increasingly being used to directly simulate the ecological processes and the global change drivers that shaped spatiotemporal patterns of biodiversity (Pilowsky et al., 2022). These new approaches in macroecology (Connolly et al., 2017) are improving knowledge of eco-evolutionary dynamics (Hagen et al., 2021), allowing contested ecological and evolutionary theories to be assessed (Rangel et al., 2018), and biodiversity to be better understood and managed (Fordham et al., 2016).

The geographic distributions of Arctic species are highly dynamic (Beumer et al., 2019), with ranges forecast to shift in future decades (van Beest et al., 2021), due to demographic processes (population growth and dispersal) responding to spatiotemporal variations in abiotic and biotic conditions (Brown et al., 1996), affecting source–sink dynamics (Gaston, 2003). Thus, making robust projections of past and future range shifts for Arctic species requires spatially explicit population models (SEPMs) that simulate metapopulation and dispersal dynamics under climate and environmental change (Anderson et al., 2009). SEPMs that directly reconstruct spatiotemporal variations in demographic change, can not only establish dynamic responses of species to climatic shifts and anthropogenic activities, but also disentangle the spatiotemporal impacts of each of these drivers (Fordham et al., 2022). This is particularly so, if spatiotemporal patterns inferred from the paleo-record and/or historical observations are used to assess whether a model is adequate in its parameterization and structure to simulate the underlying mechanisms (Fordham et al., 2016; Nogues-Bravo et al., 2018).

New approaches for reconstructing species' responses to multiple millennia of global change use inferences of demographic and distributional change from fossils and ancient DNA (aDNA) as independent, objective targets to identify whether models have the structural complexity and parameterization needed to simulate species' range shifts and extinction risk (Fordham et al., 2022). Under this pattern-oriented approach (Grimm et al., 2005), competing models are evaluated based on their ability to reconstruct biogeographical patterns inferred from paleo-archives, such as time and location of extirpation and colonization events, and changes in relative abundance (Fordham et al., 2021). This approach, which integrates the disciplines of macroecology, paleoecology, climatology, and genomics, is revealing the chains of causality that lead to species' range collapse and extinction over decades to millennia (Fordham et al., 2022).

The Arctic is an ideal system for using the past to inform contemporary conservation management and policy, because some Arctic regions experienced rates of warming that are analogous to future forecasts (Fordham et al., 2020). It also has a relatively high number of plant and animal fossils with good spatial and temporal coverage (Chevalier et al., 2020; Nogues-Bravo et al., 2018), a large volume of sequenced ancient DNA from a diverse range of species (Orlando & Cooper, 2014; Smith et al., 2003; Willerslev et al., 2003), and paleoclimate reconstructions with high temporal resolutions (Steffensen et al., 2008). Consequently, the causes of late Quaternary extinctions of Arctic megafauna have been well studied (Cooper et al., 2015; Lister & Stuart, 2008; Lorenzen et al., 2011), including, most recently, with process-explicit models and pattern-oriented validation methods (Fordham et al., 2022). However, the range dynamics of Arctic species that survived the climatically unstable Pleistocene/Holocene transition are less well understood. Here, we use process-explicit macroecological models to establish the ecological mechanisms underpinning the range dynamics of the muskox (*Ovibos moschatus*)—a cold-adapted Arctic herbivore that regulates the structure and function of tundra ecosystems (Post, 2013; Post & Pedersen, 2008)—over the last 21,000 years, to better understand the regulatory roles of climatic change and exploitation by humans on muskox abundance through space and time.

The muskox is naturally distributed in Northern Canada, Canadian Islands, and North and East Greenland, with translocated populations in Russia, Alaska (US), and Western Greenland (Cuyler et al., 2020). During the late Pleistocene, the muskox had a Holarctic distribution, stretching from Europe to North America (Markova et al., 2015). Its Eurasian range contracted during the last deglaciation [i.e., 19–11 ka BP (thousand years before present); Clark et al. (2012)], with the last surviving population going extinct ~2.6 ka BP in Taymyr (Russia; Campos et al., 2010; Markova et al., 2015). Conversely, when the range of the muskox was collapsing in Eurasia, North American populations were expanding their range on their route to colonizing Greenland (Hansen et al., 2018). Previously, warming has been suggested to be the primary driver of muskox extirpation in Eurasia, with little or no contribution of human activities such as harvesting (Campos et al., 2010; Lorenzen et al., 2011).

However, the ecological processes of range collapse of muskox in Eurasia and its range expansion in North America remain mostly a mystery, having never been reconstructed at high spatiotemporal resolutions, and not using validated process-explicit macroecological models. Here, we use a process-explicit modeling framework to (i) examine the role of climatic warming on muskox abundance and (ii) test the hypothesis that humans did not contribute to the range contraction of muskox in Eurasia during the Pleistocene, or its rate of range expansion in North America in the Holocene.

We built 100,000 plausible SEPMS that continuously reconstructed the range and population dynamics of the muskox since 21 ka BP under different conceivable levels of climate-driven resource availability and human exploitation. Models that could reconcile inferences of demographic change from fossils were identified using pattern-oriented methods (Grimm & Railsback, 2012) and used to determine the likely chains of causality responsible for the contemporary distribution of muskox. Simulations from these validated models were analyzed statistically to better establish the drivers responsible for the extinction of muskox in Eurasia and its range expansion in North America. We show that climatic change was probably the primary driver of the structure and dynamics of the geographic range of muskox, with human activities, and their interactions with climatic changes, being important in some regions.

## 2 | MATERIALS AND METHODS

We built process-explicit macroecological models of muskox that simulate interactions between metapopulation dynamics, climate variability, and hunting by humans (Figure 1). We used these models to continuously reconstruct 21,000 years of range contraction and expansion across Eurasia and North America. We refined the parameter space of our simulations of spatiotemporal abundance with pattern-oriented methods (Grimm & Railsback, 2012), using inferences of range shifts, extirpation, and colonization events estimated from hundreds of fossils. The approach is described in detail in the Supplementary Methods. Supporting appendices can be found in Canteri et al. (2022), including the fossil and modern occurrence record (Appendix 1), the R code for running the models (Appendix 2) and a table explaining the variables used for the statistical analysis (Appendix 3).

### 2.1 | Ecological niche

To reconstruct the ecological niche of the muskox through space and time, we intersected radiocarbon dated and georeferenced fossils, and modern observations of muskox, with gridded climatic data: paleoclimate reconstructions and interpolated current-day climate observation.

Fossils from the Late Pleistocene and Holocene were compiled from publicly available databases and published literature (see Supplementary Methods). The quality and reliability of all

radiocarbon dates were assessed (Barnosky & Lindsey, 2010) and only fossils with an age quality score  $>10$  were used. The radiocarbon ages of these fossils were calibrated using OxCal and the IntCal20 calibration curve (Bronk Ramsey, 2009; Reimer et al., 2020). This resulted in 135 reliable fossil ages with geolocations and calibrated ages younger than 21 ka BP: the limit of our high temporal resolution paleoclimatic data (Figure S1; Appendix 1). Fossil data were supplemented with modern occurrence observations for muskox in North America for the period 1700AD–2019AD (Figure S1; Appendix 1). These records were retrieved from GBIF (GBIF.org, 2019).

Occurrence records from observations and fossils were intersected spatiotemporally with seven climatic variables: average minimum daily temperature in January, average maximum daily temperature in January, average maximum daily temperature in July, precipitation seasonality, annual precipitation, temperature seasonality, and evapotranspiration in spring and summer. Paleoclimate data came from the TraCE-21ka simulation (Liu et al., 2009) accessed through PaleoView (Fordham et al., 2017) and is described in detail in Fordham et al. (2017). Independent validation shows that the TraCE-21ka simulation closely reproduces inferences of temperature change over the last 21,000 years (Brown et al., 2020; Liu et al., 2009). Because TraCE-21 data are not available after 1989AD, we harmonized recent climate observations from CRU TS v4 (Harris et al., 2020) with the TraCE-21ka simulation using the change factor method (Beyer et al., 2020). All climate data were resampled to a  $1^\circ \times 1^\circ$  resolution. Climate variables were tested for collinearity. Three variables with  $|r| < 0.7$  (Dormann et al., 2013) were retained for modeling the ecological niche of the muskox: average minimum daily temperature in January, annual precipitation, and total evapotranspiration in spring and summer. These three climatic variables have been used previously to model the range dynamics of large vertebrates in Eurasia (Lorenzen et al., 2011; Nogués-Bravo et al., 2010; Yannic et al., 2014, 2020). These climatic variables are important distal predictors for arctic grazers, as they influence plant community composition and primary productivity, and thus forage availability and quality, which ultimately affect vital demographic rates and muskox population dynamics (Asbjornsen et al., 2005; Desforges et al., 2021). While important proximal predictors, such as snow depth and snow conditions (Asbjornsen et al., 2005; Desforges et al., 2021), were considered, they are difficult to simulate at a Holarctic scale (Foster et al., 1996), particularly over paleo time scales.

The climate occurrence data were used to build a three-dimensional hypervolume of climate suitability through time (Nogués-Bravo, 2009), generating a biologically relevant representation of the climatic conditions over which the muskox occurred at fossil and modern occurrence sites. We built a Gaussian hypervolume of climate suitability using the “hypervolume” R package (Blonder et al., 2014). We tuned the kernel density estimation (KDE) bandwidth using cross-validation (Blonder et al., 2014). We used the “hypervolume” package because it does not require absence data and because it generates projections that are less sensitive to extrapolation (Blonder et al., 2017).

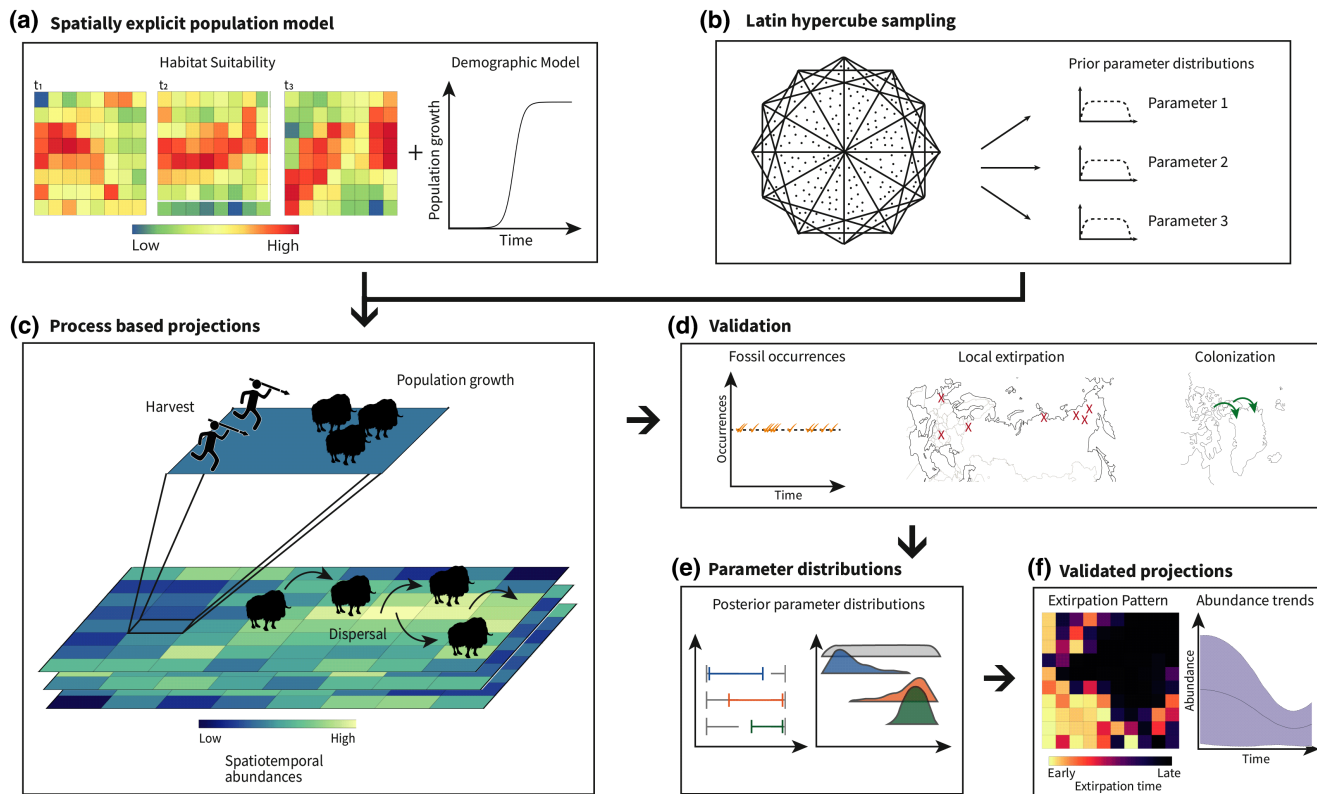


**FIGURE 1** Modeling the range dynamics of muskox using spatially explicit population models. Spatially explicit population models (SEPMs) account for spatiotemporal change in habitat suitability and demography (a). Uncertainty in climate–human–muskox interactions is modeled by generating thousands of models with unique combinations of parameter values sampled from wide but plausible ranges, using Latin Hypercube sampling (b). Each model simulates changes in spatiotemporal abundance in response to climatic change and hunting by humans (c). Model projections are validated using Approximate Bayesian Computation and pattern-oriented methods, which compare observed or inferred patterns (targets) to simulated patterns (d). Prior and posterior distributions can be visualized to identify important model parameters (e). A subset of “best” models can be used to generate validated projections of abundance and extinction dynamics (f).

The resulting hypervolume, which approximates the fundamental niche of the muskox (Nogués-Bravo, 2009), was exhaustively subsampled to generate thousands of potential realized niches (Fordham et al., 2022). Subsampling of the niche was done using Outlier Mean Index (OMI) analysis (Dolédéc et al., 2000), using plausible bounds of climatic specialization and niche breadth (Fordham et al., 2022). For each niche subsample ( $n = 2500$ ), we generated spatial projections of climate suitability from 21ka BP to 1500AD at 8-year generational time steps. This allowed the realized niche of the muskox to be identified using process-explicit macroecological modeling (described below). Methods used to model the ecological niche of the muskox are described in detail in the Supplementary Methods.

## 2.2 | Human relative abundance

Relative abundance and expansion of humans in Eurasia and North America was modeled using a Climate Informed Spatial Genetics Model (CISGeM; Eriksson et al., 2012). Pattern-oriented modeling (POM) has shown that CISGeM can accurately reconstruct arrival times of anatomically modern humans and current-day distributions of effective population sizes ( $N_e$ ; Eriksson et al., 2012; Raghavan

et al., 2015). This is done in CISGeM by modeling local  $N_e$  as a function of genetic history, local demography, paleoclimate, sea level, and net primary productivity over the last 125k years (Eriksson et al., 2012; Raghavan et al., 2015).

Arrival time, occupancy, and density (here  $N_e$ ) of humans were forced in CISGeM by spatiotemporal estimates of climate, sea level changes, and ice sheet dynamics over the past 125k years, operating at 25-year time steps. To do this, climate data from the HadCM3 global circulation model prior to the last glacial maximum were harmonized with TraCE-21 data (Fordham et al., 2022). To account for parameter uncertainty in spatiotemporal projections of  $N_e$ , we used published upper and lower confidence bounds for CISGeM parameters (Eriksson et al., 2012) to generate ~4000 different plausible models of human migration (each with a unique combination of parameters), using Latin hypercube sampling (McKay et al., 1979). We rejected model simulations that were unable to successfully replicate arrival times in North America. We then calculated the multi-model mean and standard deviation for each grid cell at each time step in the model from 21ka BP and used this information to generate 100,000 potential human migration and population growth scenarios (Fordham et al., 2022). All  $N_e$  values were scaled between 0 and 1 (using the 95th percentile of the values from the

multi-model mean) and used as a measure of relative abundance of humans in the process-explicit macroecological model (Fordham et al., 2021). CISGeM and its application are described in detail in the Supplementary Methods.

### 2.3 | Climate–human–muskox interactions

The range dynamics of the muskox were simulated using a SEPM framework (Fordham et al., 2021). Demographic processes (population growth, dispersal, source–sink dynamics, and Allee effect) were simulated as dynamically responding to changing climatic conditions, human harvesting, and their interactions, from 21 k BP until 1500 AD. We did this using lattice-based stochastic demographic models, operating at a generational time step of 8 years (Hansen et al., 2018). These process-explicit models have been shown to be successful at projecting the range dynamics of species (Fordham et al., 2018, 2021), including extinct megafauna (Fordham et al., 2022). SEPMs were built using the “poems” and “paleopop” R packages (Haythorne, Fordham, et al., 2021; Haythorne, Pilowsky, et al., 2021).

Driver–state relationships simulated the effects of climatic change and hunting by humans on key ecological processes of extinction: lability of the ecological niche, dispersal, population growth, and Allee effect. Dispersal was simulated using a distance-based function that limited movement to resource-depleted areas, and blocked movement across grid cells covered by sea or glacial ice (Fordham et al., 2021). Carrying capacities and initial abundances were generated as a function of habitat suitability (i.e., availability of resources; Fordham et al., 2018), and proportion of glacial ice present in a grid cell. We modeled density-dependent growth using a logistic function (Ricker, 1954). Harvesting was modeled as a function of prey density, human density, exploitation rate, and prey availability (Alroy, 2001; Fordham et al., 2022). An Allee effect was used to simulate rapid extinction at small population size (Fordham et al., 2013).

Models were parameterized using best estimates for demographic processes (population growth rate and variance, dispersal, Allee effect), environmental attributes (niche breadth and climatic specialization), and threats (human abundance and exploitation rate). Values for these processes were varied across biologically plausible ranges (Table S1), using Latin Hypercube sampling of uniform probability distributions (Fordham et al., 2021). This resulted in 100,000 conceivable model parametrizations, each with different demographic processes and rates of climate change and exploitation by humans. Each model was run for a single replicate (Prowse et al., 2016). The process-explicit model is described in detail in the Supplementary Methods.

### 2.4 | Pattern-oriented modeling

We used POM to validate model simulations and optimize model parameters (Grimm et al., 2005). The capacity of models to replicate

inferences of occupancy, extirpation, and colonization events from the fossil record was tested using Approximate Bayesian Computation (ABC) analysis (Csilléry et al., 2010). We did this using a multivariate validation target, consisting of occupancy at fossil sites ( $\text{age} \pm 1 \text{ SD}$ ), arrival time in Greenland, timing of regional extirpation in Eurasia, and distance from extinction location in Eurasia. Estimates for these targets are in Table S2.

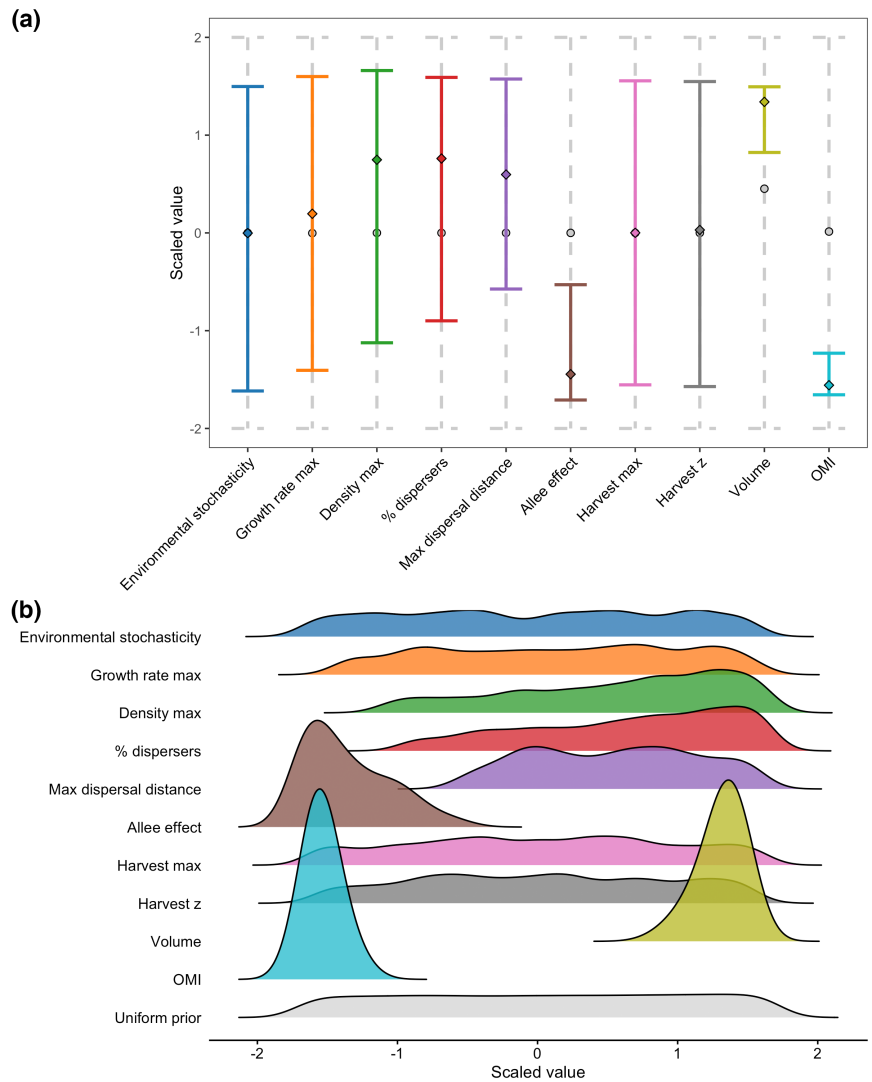
We used POM and ABC to identify and select the top 1% of model simulations ( $n = 1000$ ) that most closely replicate the validation targets. We did this using the rejection method (Csilléry et al., 2012). We calculated the parameter distributions of selected models (i.e., posterior distribution) and compared them with their prior ranges (van der Vaart et al., 2015). We mapped muskox abundance in space and time using an ensemble average of the selected simulations (weighted by the Euclidean distance from the targets) and calculated timing of extirpation and change in total and regional population size. The regions were Europe, with the Ural Mountains defining the eastern boundary; Asia, between the Urals and the Lena River; Beringia, between the Lena River and Alaska; and North America, encompassing Northern Canada and Greenland (Fordham et al., 2022; Table S2). All multi-model average reconstructions of spatiotemporal abundance accounted for probability of occurrence and Allee effect (Fordham et al., 2022). The POM methods are described in detail in the Supplementary Methods.

We compared changes in relative total population size (effective population size) from aDNA with change in relative total population size from the “best” models selected using POM validation procedures. The methods and data used to calculate effective population size are described in the Supplementary Methods. This secondary test, using independent targets, tested whether the “best” models, did indeed adequately capture the ecological processes of range dynamics and their driver–state relationships (Grimm & Railsback, 2012). The correlation between the simulated trends in total abundance for the selected models and abundance trends inferred from aDNA was calculated. We also compared magnitudes of change in relative population size for the last deglaciation (19–11 ka BP) and Holocene (11 ka BP–1500 AD) across both groups. To do this, we calculated the magnitude of change in abundance between the start and end, of the last deglaciation, and the start and end of the Holocene, for each of the selected models and for an equivalent number of uniformly sampled points within the 95% CI of the  $N_e$  trend at those specific time points. We then did a Welch's *t*-test to determine if there were significant differences in magnitude of change for each period between the aDNA and our simulations.

### 2.5 | Statistical analysis

We used machine learning techniques to statistically identify and distinguish the relative effects of climate and humans on the extinction risk of the muskox during the last deglaciation period. For the selected simulations, we calculated five spatiotemporal descriptors for climatic change and five spatiotemporal descriptors for human

**FIGURE 2** Prior and posterior distributions for modeled parameters. (a) Shows scaled parameter ranges for prior (broken line) and posterior (colored line) parameters in the muskox SEPM. Circles and diamonds represent the mean of the prior and posterior distributions, respectively. Raw values for prior and posterior parameter ranges are provided in Table S1. (b) Shows the density of the posterior distribution compared to a uniformly distributed prior. Variable demographic parameters in the muskox SEPM are variation in population growth rate (Environmental stochasticity); maximum population growth rate (Growth rate max); proportion of individuals dispersing at each time step (% dispersers); maximum dispersal distance (Max dispersal distance); Allee effect; and maximum abundance (Density max). Variable harvest parameters are percentage of the population that is harvested (Harvest max); extent to which harvest follows a Type II to Type III functional response (Harvest z). Variable parameters describing ecological niche requirements are distance between the climatic conditions of the occupied and potential fundamental niche (OMI, Outlier Mean Index), and breadth of climatic conditions the species can occupy (Volume).



harvesting (these are described in detail in Appendix 3, Canteri et al., 2022) at the regional level. We calculated expected minimum abundance (EMA) during the last deglaciation for Asia, Beringia, and North America, which is a measure of risk of population decline and extinction (McCarthy & Thompson, 2001). We used time to extinction in Europe instead of EMA, because the muskox went extinct before the end of the last deglaciation in Europe (Table S2). We used a similar approach to assess the roles of climate and human harvesting during the Holocene (stopping at 1500AD) on population abundance of muskox in North America and East Beringia (Alaska, USA) in 1500AD (i.e., the end of the simulation).

Random forest classification trees, implemented with the “ranger” package in R (Wright & Ziegler, 2017), were used to statistically identify spatiotemporal effects of climate and human drivers on EMA and time to extinction. We constructed 1000 trees and tuned the number of variables and minimum node size at each split via 10 × 10-fold cross-validation, to maximize model accuracy. Variable importance scores were calculated using unscaled permutation importance (Strobl et al., 2007) and converted to % contribution of the variance explained.

### 3 | RESULTS

Based on the multi-model ensemble average of the best 1% of plausible SEPMs, the muskox is projected to have declined in population size and contracted their range in a northeasterly direction in Eurasia during the last deglaciation (Figures 3 and 4); and to have expanded its populations in North America (north of 50° latitude) during the Holocene, colonizing Greenland (Video S1). These “best” models, according to POM methods, correctly projected spatiotemporal occurrence in up to 96% of fossil sites ( $94 \pm 11$ ) and predicted the timing of extirpation (particularly in Europe; Figure 4) and the distance from the last fossil in Eurasia (Figure S5) with good accuracy (RMSE:  $324 \pm 83$ ; distance from extinction location:  $1161 \pm 241$  km). However, they did predict a mean arrival time in Greenland that is ~2 k years earlier than expected from the current fossil record (Figure S5).

Validation using genetic inferences of change in total population size showed that projections of total population size for the best SEPMs matched changes in population size inferred from ancient DNA reasonably closely ( $\bar{r} = 0.64 \pm 0.07$ ). Both reconstructions

show a steep decline in total population size at the beginning of the deglaciation period, stabilization, and then an increase during the Holocene (Figure S6). The means of the slopes for magnitude of change in relative population size between selected simulations (mean slope =  $-0.0000188$ ) and those inferred from  $N_e$  (mean slope =  $-0.0000193$ ) were not significantly different for the last deglaciation [ $t(1955.6) = 0.99, p = .32$ ]. However, they were significantly different in the Holocene [ $t(1334.3) = -25.53, p < .001$ ], with our selected simulations (mean slope =  $0.0000203$ ) showing an earlier increase in relative population abundance compared to the estimates from  $N_e$  (mean slope =  $0.0000385$ ) as shown in Figure S6.

### 3.1 | Demographic and ecological processes

To reconstruct inferences of past demographic changes from fossils, SEPMs for muskox required large maximum densities, high dispersal abilities (a high proportion of dispersing individuals, with a long dispersal tail), and small Allee effects (Figure 2). Moreover, the ecological niches of muskox needed to have large volumes and low specialization, with selected niches closely approximating the fundamental (multi-temporal) niche of the muskox. The posterior distribution of some parameters more closely matched their prior distribution (Figure 2), suggesting a lesser role in the structure and dynamics of the geographic range of the muskox. These non-identifiable parameters included some demographic parameters (environmental stochasticity and maximum growth rate) and parameters linked to harvesting by humans [exploitation rate (Harvest Max) and prey functional response (Harvest z)].

### 3.2 | Structure and dynamics of the geographic range

Our simulations accurately reconstructed inferences of the past distribution, extirpation, and abundance of the muskox over the last 21k years. Multi-model averaged estimates of timing of extirpation (Figure 3a) show a range collapse in Eurasia in a north-eastward direction, with severe and wide-scale population declines occurring after large magnitude and rapid warming at  $\sim 14.7$  ka BP (Figure 4). Populations in central Europe are projected to have gone extinct before 17ka BP, persisting in north-eastern Europe until  $\sim 13$ ka BP, which is in strong agreement with the fossil record (Figure S5). While population abundances of muskox in north-eastern Europe are projected to have declined sharply following the 14.7 ka BP warming event, our simulations suggest that their regional extinction in Europe occurred during a secondary warming phase, immediately following the 14.7ka BP event (Figure 4).

In North America, populations that persisted during the last glacial maximum south of the Laurentide ice sheet, are projected to have moved in a northerly direction from 17ka BP in response to melting of the ice sheet (Video S1), going extinct south of the ice sheet at approximately 13ka BP (Figure 3). From 14.5 ka BP, populations

in Alaska migrated toward the Canadian Arctic Archipelago and Greenland (Video S1), colonizing much of North America north of  $65^\circ$  in latitude. North America north of  $55^\circ$  in latitude is projected to have been colonized by 6 ka BP (Video S1). The simulated distribution of muskox in North America in 1500AD (Figure 3b; the end of the simulation) aligns closely with the current endemic distribution of muskox (Figure 3c), with the southern boundary of the simulated distribution matching the southern boundary of today's non-translocated range.

In Asia and Beringia, the distribution of the muskox is projected to have contracted in a northerly direction, with animals being isolated in fragments by 13ka BP, and with populations persisting at low densities in Siberia and Beringia until 1500AD (Figure 3b). Our models project persistence in Asia at 1500AD, which does not align with fossil evidence of regional extinction at  $\sim 2.6$  ka BP. However, the areas where these populations are projected to have persisted in low numbers are the same areas where muskox have been recently translocated (Figure 3c; Cuyler et al., 2020).

The total population size of muskox is projected to have declined during the last deglaciation period (19–11 ka BP) and then increased during the Holocene (Figure 4) owing to range expansion in North America. The largest declines in regional population size occurred during or immediately following the 14.7 warming event, where regional temperatures warmed at rates of up to  $3^\circ\text{C}$  per century (Figure 4). In North America, the population size of muskox also declined with an abrupt increase in temperature at around  $\sim 7$  ka BP.

### 3.3 | Climate–human–muskox interactions

Climatic changes explained 62%, 74%, and 45% of the variance in EMA during the last deglaciation period in Asia, Beringia, and North America, respectively (Figure 5). There was minimal evidence for an impact of activities of humans on EMA in these three regions prior to the Holocene, with human parameters explaining only 0.4%, 1.4%, and 2.3% of the variance (Figure 5). Large contractions in climate suitability and a faster pace of loss in suitable climatic conditions resulted in lower EMA in Asia (Figure S8). In Beringia and North America, a northern movement of climate suitability positively influenced EMA, while large changes in climate suitability had a negative effect (Figures S9 and S10).

Post-simulation statistical analysis of time to extinction in Europe showed that the effects of climate and humans were similar, explaining 13% and 10% of the variance, respectively. Timing of extinction occurred sooner in simulations where climate suitability in Europe declined quicker in a westerly direction, and where humans expanded slowly in a northerly direction following the last glacial maximum (Figure S7).

In Eastern Beringia (Alaska, USA), climate change had the largest influence on simulated abundance during the Holocene. Climatic change explained 17% of the variance in muskox population size in 1500AD in Eastern Beringia, with humans explaining  $<1\%$  of variance. Abundance in Eastern Beringia was negatively influenced

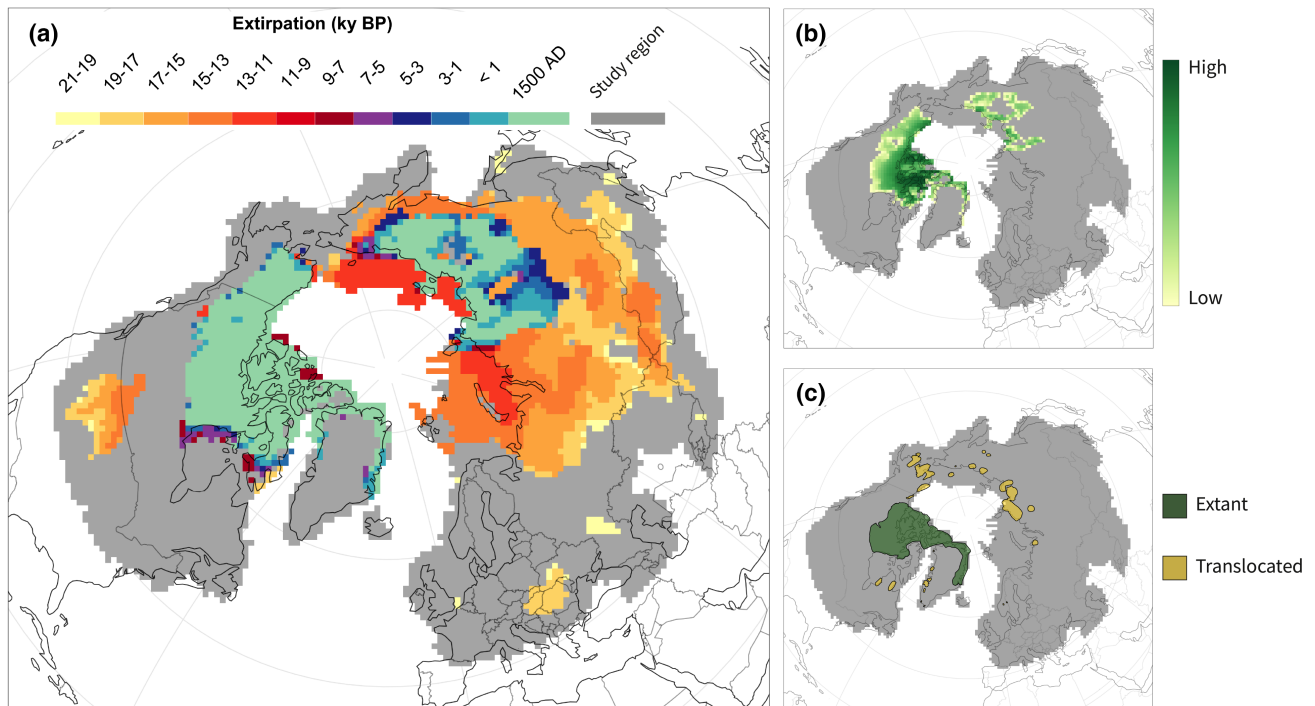


**FIGURE 3** Change in the distribution of muskox over the last 21,000 years. Projected time of extirpation of muskox (a). Areas simulated to be occupied in 1500AD, with their relative densities (b). Panel (c) shows the current natural distribution of muskox (extant), and where muskox have recently been translocated for conservation purposes (Cuyler et al., 2020).

by large changes in climatic conditions (shifting in a north-east direction), slow paces of increased climatically suitability, and large amounts of habitat fragmentation (Figure S11). While in North America (excluding Alaska), humans and climate are likely to have been equally important drivers of abundance during the Holocene (Figure 6). Climatic changes during the Holocene explained 7.8% of the variance in muskox population size, while indices of human activities explained 8.2%. Population size at 1500AD was negatively correlated with human expansion (magnitude and pace) during the Holocene and the degree to which climate suitability shifted in a southerly direction during this period (Figure S12). A lower explained variance for Holocene models is expected because climate–human–muskox interactions during the Holocene are affected by climate and human processes happening before the Holocene (Figure 5), which are not directly considered in this analysis.

## 4 | DISCUSSION

Spatially explicit population models that continuously simulate climate–human–muskox interactions indicate that the population structure and range dynamics of muskox have been shaped by deglacial climatic change, with rapid warming events causing population crashes and range contractions. Conversely, more stable climatic conditions during the Holocene enabled the populations of muskox in North America to grow and expand. Human activities, including harvesting, are likely to have operated in synergy with climatic change to affect abundances of muskox in some regions,

contributing to its extirpation in Europe approximately 12,000 years ago, and to its contemporary population structure in North America. We show that reconciling past inferences of demographic changes from the fossil record and aDNA requires specific demographic and niche constraints, and regional variations in rates of climatic change, exploitation by humans, and their interaction.

Differences between the posterior and prior distributions of SEPM parameters indicate that long-distance dispersal and meta-population processes, and their interactions with climatic change and human activities, are important ecological mechanisms driving the structure and dynamics of the geographic range of the muskox. The role of human activities in driving muskox population dynamics has previously been rejected, due to low numbers of muskox remains at archaeological sites (Lent, 1999). This has been interpreted as indicating small levels of range overlap between muskox and Paleolithic humans (Lorenzen et al., 2011). However, our simulations show that the ranges of Paleolithic humans and muskox are likely to have overlapped in Eurasia for long periods of time during the most recent deglacial period (Video S2), with humans probably having a pronounced effect on population abundances in areas more densely populated by humans, such as Europe (Fordham et al., 2022). These impacts on muskox populations by humans are likely to have been both direct (i.e., through hunting) and indirect, with humans regularly occupying pathways between resource-rich zones, potentially hindering important metapopulation processes (Cooper et al., 2015).

We show that simulating inferences of demographic change from fossils and aDNA requires a northeasterly contraction of the Eurasian range of the muskox during the late Pleistocene and an expansion



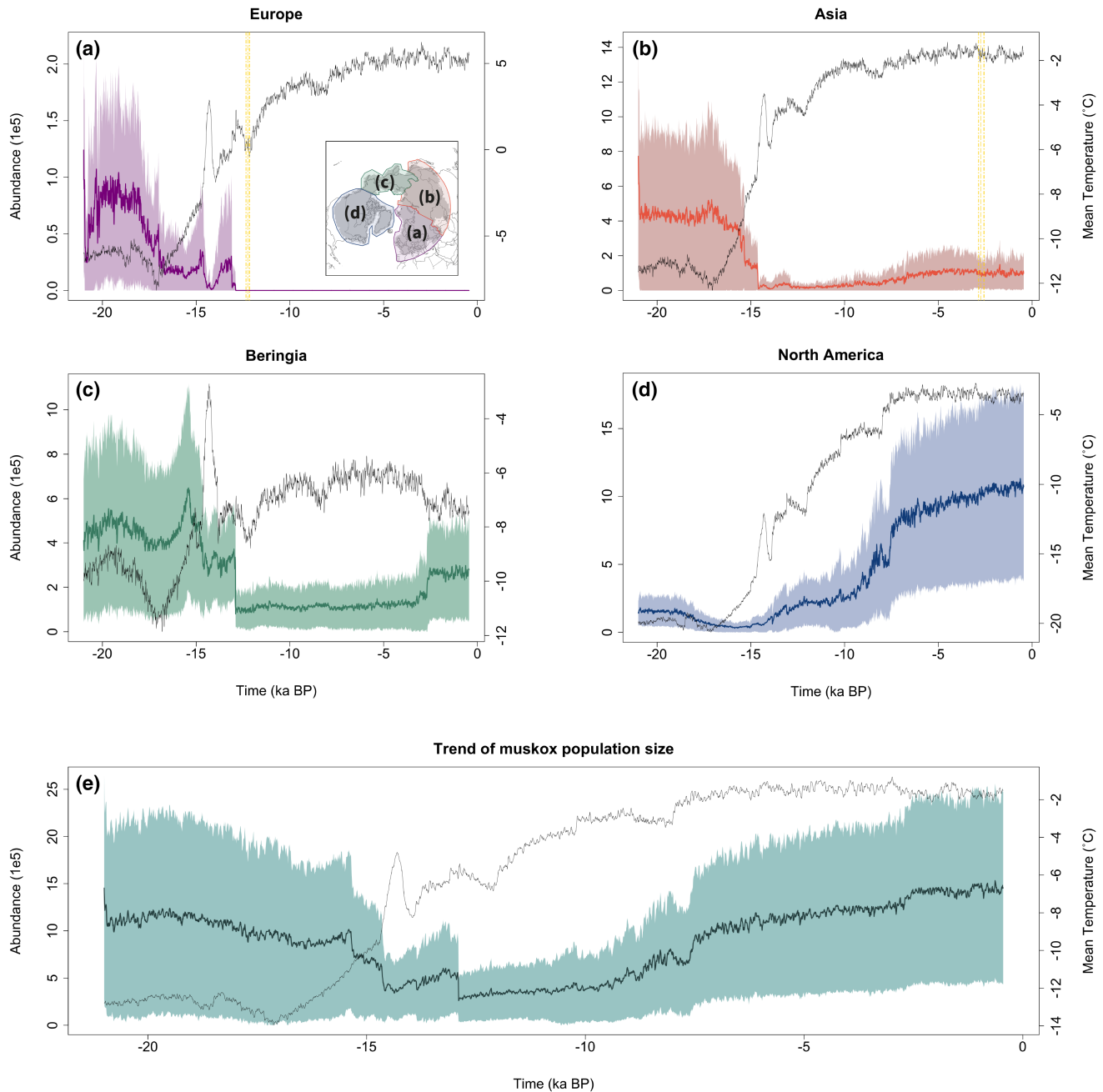
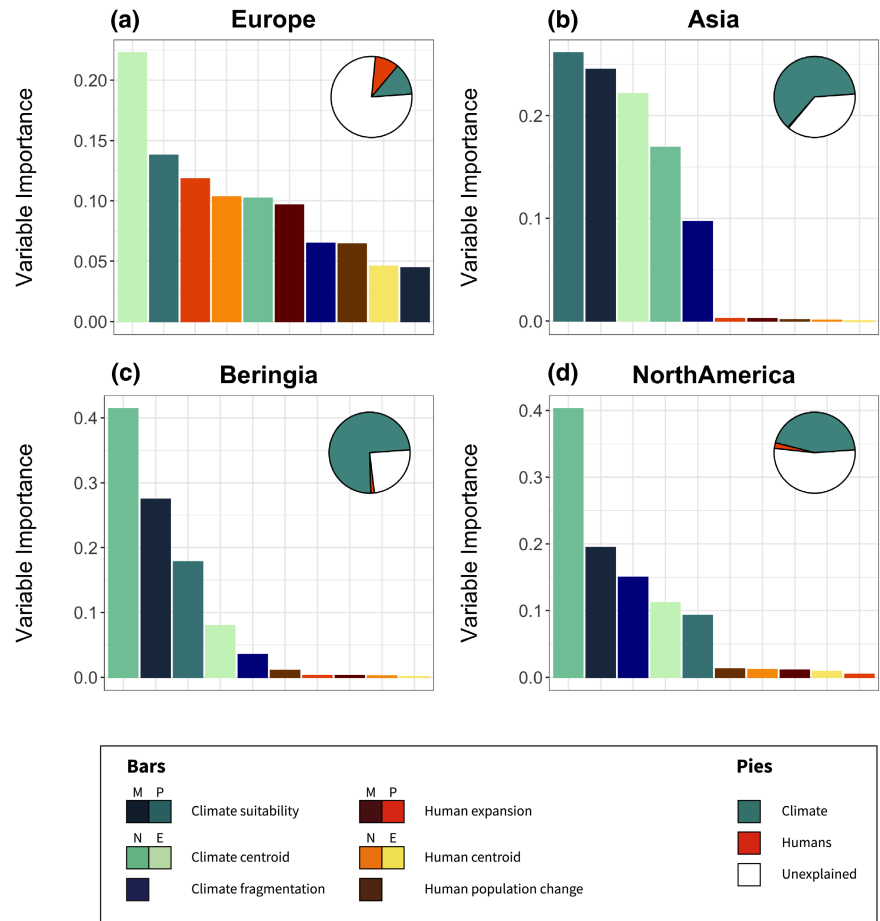


**FIGURE 4** Temporal changes in population size. Total population size (mean abundance  $\pm 1$  SD; left y axis; colored lines) and mean annual temperature (thin black line; right y axis) since 21 ka BP simulated for Europe (a), Asia (b), Beringia (c), North America (d) and for its once entire Holarctic range (e). The geographical division of sub-regions is shown in the inset of panel (a). The yellow vertical lines represent time of extinction based on the fossil record.

of its range and abundance in North American during the Holocene. Simulated population sizes of muskox declined abruptly in response to the Dansgaard–Oeschger warming event (~14.7 ka BP), when temperatures increased by as much as 10°C in <50 years (Dansgaard et al., 1993), signaling a vulnerability of muskox to abrupt climatic warming. This and other abrupt warming events of the Pleistocene (Botta et al., 2019) caused severe range contractions and population crashes for other megafaunal species, including the Cave lion (Stuart & Lister, 2011), woolly rhinoceros (Lord et al., 2020; Stuart & Lister, 2012), and woolly mammoth (Fordham et al., 2022; Stuart & Lister, 2012).

These rapid warming events are likely to have affected snow conditions, and more specifically snow accumulation, negatively impacting the breeding success and survival of the muskox (Desforges et al., 2021). They are also likely to have altered wind and precipitation patterns, intensifying the frequency of rain-on-snow events, which today prevent Arctic ungulates from accessing food, increasing mortality (Berger et al., 2018). Following the termination of the Pleistocene, population sizes of muskox increased, resulting in simulated population sizes at 1500 AD that were like those at the height of the last glacial maximum (Figure 4e).

**FIGURE 5** Effects of climate and humans on muskox abundance at the termination of the last deglaciation. Drivers of time to extinction in Europe (a), and of expected minimum abundance (EMA) at 11 ka BP in Asia (b), Beringia (c), and North America (d). Bars represent individual contributions of measures of climatic change and human activities on explained variance in EMA or time to extinction. Variables are divided into magnitude (M) and pace (P) of change in climate suitability and human expansion, movement north (N) and east (E) of core climate suitability (climate centroid) and human abundance (human centroid), amount of fragmentation in climatically suitable areas (climate fragmentation), and growth in the human population (Human population change). All variables are explained in detail in Appendix 3 (Canteri et al., 2022). Pie charts show the variance explained (%) by climate (blue) and humans (red). White areas in the pie charts represent unexplained variance.



Population growth and range expansion was a feature of muskox range dynamics in North America during the Holocene, owing to more gradual rates of warming compared to the Pleistocene. However, populations crashed at ~7 ka BP in our simulations, probably in response to temperatures being as warm or warmer than today (Kaufman, 2004; Wanner et al., 2008).

Our simulations of range contraction for muskox in Eurasia during the Pleistocene align with existing vegetation reconstructions and vegetation models, showing that the shrub and steppe tundra biomes, preferred by the muskox, became fragmented and were gradually replaced by temperate and boreal forests, as a result of warmer and wetter climatic conditions (Allen et al., 2020; Binney et al., 2017). Furthermore, our models correctly simulate the expansion of muskox in North America from Alaska to the northern part of Canada, Canadian Islands, and into Greenland. This pattern is supported by genetic data, which shows signs of multiple founder effects during the colonization of the Canadian Arctic Archipelago and Greenland (Hansen et al., 2018); and fossil data, suggesting that the species entered Greenland from Ellesmere Island via the Nares Strait (Bennike, 1999). In North America, a moisture gradient shift in the tundra biome toward wetter conditions, following the retreat of the Laurentide ice sheet starting at 14 ka BP, favored mesic specialists like muskox and reindeer, while dryland specialists like horse, bison, and mammoth went extinct (Mann et al., 2013).

Tundra is the preferred habitat of muskox (Beumer et al., 2019; Schmidt et al., 2016), where it consumes a wide variety of plants (Kristensen et al., 2011; Schmidt et al., 2018). In Europe, climate-driven transformation of tundra to forest vegetation began at the onset of the deglaciation period, being complete by 13 ka BP (Binney et al., 2017). While the timing of this transformation in vegetation coincides with our projections of population declines in Europe, and its later extinction from the region, we show that humans are likely to have played an additional and important role in the extirpation of muskox in Europe. Measures of human activities had nearly as strong an influence on the simulated timing of extirpation in Europe as did measures of climatic change. Thus, a synergy between human activities and climate-induced vegetational changes likely hastened the extinction of muskox in Europe during the late-Pleistocene.

A comparison of the effects of climate and humans during the Holocene on muskox abundance in North America also shows that human activities, as well as climatic change, probably shaped the structure and size of muskox populations. Muskox remains are more frequently associated with Holocene-age human artifacts in North America, potentially indicating a more specialized muskox-hunting culture in this region following the Holocene (Lent, 1999), which our results corroborate. Furthermore, it is hypothesized that humans reached Greenland by following the muskox, using the so-called "Muskox Way" (Lent, 1999), suggesting that muskox played

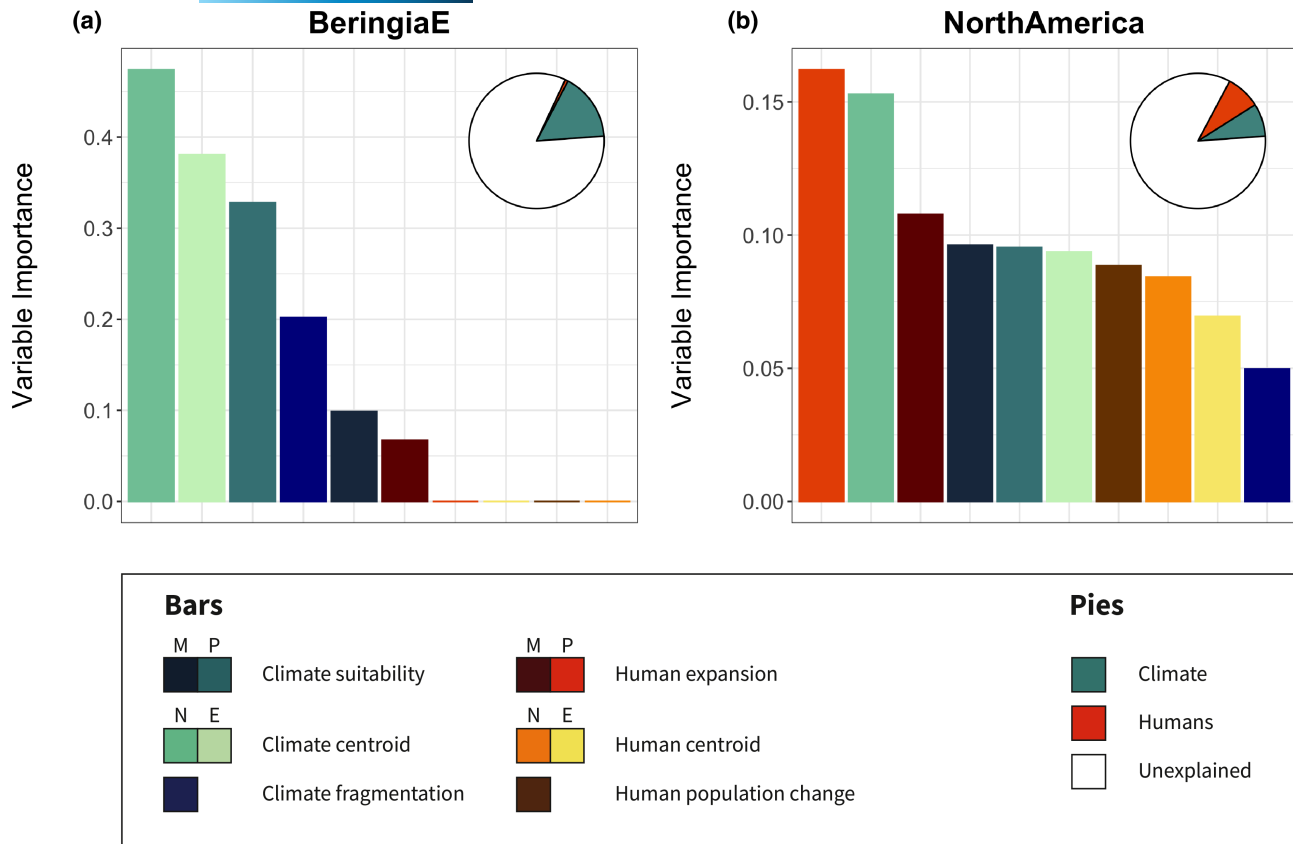


**FIGURE 6** Effects of climate and humans on muskox final abundance. Drivers of final abundance in Eastern Beringia (Alaska, USA) (a) and North America (b) during the Holocene. Bars represent individual contributions of measures of climatic change and human activities on explained variance in population size at 1500AD. Pie charts show the variance explained (%) by climate (blue) and humans (red). White areas in the pie charts represent unexplained variance. See Figure 5 for further details.

an important role in the establishment of humans in Arctic North America and, subsequently, in Paleo-Inuit culture.

While our process-explicit models do well at reconstructing inferences of range shifts and demographic change from fossils, they were unable to simulate the extinction of muskox in Eurasia at ~2.6 ka BP (Campos et al., 2010; Markova et al., 2015). Rather they simulate persistence of muskox in areas of Siberia (its last refuge in Eurasia) where they have been recently translocated and where populations are currently increasing (Cuyler et al., 2020). Although it is likely that the muskox went extinct in Eurasia after 2.6 ka BP (Wang et al., 2021), it is unlikely that they would have been in Eurasia during the 16th century as projected by our model. Possible reasons for simulating prolonged persistence in Siberia include an absence of inter-specific interactions in the model, other than muskox–human interactions. Bears and wolves, which are primary predators of muskox (Heard, 1992; Reynolds et al., 2002), could have amplified the effect of Holocene warming on muskox persistence in Eurasia. Moreover, our SEPM for muskox does not account for land use change during the Holocene, where pastoralism and agriculture began as early as 4 ka BP in Siberia (Stephens et al., 2019). It also does not account for potential diseases. Infectious diseases and pathogens have caused recent population declines of muskox of up to 85% in Alaska and Canada (Cuyler et al., 2020), with the range dynamics of common pathogens being sensitive to climatic warming (Kafle et al., 2020).

We project a time of arrival in Greenland that on average is approximately 2000 years earlier than the time estimated from the fossil record (~5 ka BP). This could be because our models are coarse, resulting in overly high connectivity between the Canadian Arctic Archipelago and Greenland, preventing isolation between populations, as determined by their genetic structure (Hansen et al., 2018). However, there is also a real possibility that muskox did colonize Greenland earlier than previously thought and that older fossils are still yet to be discovered. Extirpation and extinction events of megafaunal species are commonly revised as younger fossils and environmental DNA are discovered, often causing persistence to be extended by several millennia (Haile et al., 2009; Murchie et al., 2021; Wang et al., 2021). Because the fossil record indicates when a species was abundant (Bradshaw et al., 2012), it is possible that Greenland was colonized at 7 ka BP (as predicted by our models), but abundances remained low until ~5 ka BP, when the first muskox fossils appear in the fossil record. Indeed, ice-free areas of Greenland were occupied by reindeer at ~9 ka BP, long before the estimated arrival date for muskox (Meldgaard, 1986).

While our model was able to simulate important demographic changes, it was not able to account for the effect of demographic factors operating at finer spatial scales. These include, but are not limited to, narrow intervening bodies of open water in the Canadian Arctic Archipelago, which are likely to have influenced dispersal capacity. Such factors could impact important aspects of muskox biology, as

indicated by high genetic differentiation observed between populations in the Canadian mainland, Canadian Arctic Archipelago, and Greenland (Hansen et al., 2018). Moreover, our SEPMs of the range and population dynamics of muskox could potentially be improved through the use of multiple paleoclimate simulations (Fordham et al., 2011).

Using SEPMs, integrated with inferences from fossils and aDNA, we were able to disentangle the ecological mechanisms and drivers likely to have been responsible for the range collapse of muskox in Eurasia during the late Pleistocene and its expansion in North America during the Holocene. We show that while the structure and dynamics of the geographic range of muskox has been shaped by climate at the circumpolar scale, the activities of humans probably affected the range and extinction dynamics of muskox in particular regions, at particular times. We also show that muskox populations are likely to have crashed during periods of rapid warming and in ancient warm periods. Given that these Arctic warming events are directly comparable to 21st century projections (Fordham et al., 2020), our results suggest a high vulnerability of muskox to future climate warming. More generally, our process-explicit models, optimized and validated on inferences of past demographic change from fossils and aDNA, provide a new validated modeling framework for conserving muskox and other Arctic grazing megafauna under future climatic and environmental change, including pinpointing new sites for translocations.

## ACKNOWLEDGMENTS

This project was funded by an Australian Research Council Discovery Project (DP180102392) and by the Danish National Research Foundation (DNRF96). Open access publishing facilitated by The University of Adelaide, as part of the Wiley - The University of Adelaide agreement via the Council of Australian University Librarians.

## CONFLICT OF INTEREST

The authors declare no conflict of interest for this article.

## DATA AVAILABILITY STATEMENT

The data that support the findings of this study are openly available in "Dryad" at <http://doi.org/10.5061/dryad.3r2280gjj>.

## ORCID

Elisabetta Canteri  <https://orcid.org/0000-0001-9867-8247>

Stuart C. Brown  <https://orcid.org/0000-0002-0669-1418>

Niels Martin Schmidt  <https://orcid.org/0000-0002-4166-6218>

Rasmus Heller  <https://orcid.org/0000-0001-6583-6923>

David Nogués-Bravo  <https://orcid.org/0000-0002-4060-0153>

Damien A. Fordham  <https://orcid.org/0000-0003-2137-5592>

## REFERENCES

- Allen, J. R. M., Forrest, M., Hickler, T., Singarayer, J. S., Valdes, P. J., & Huntley, B. (2020). Global vegetation patterns of the past 140,000 years. *Journal of Biogeography*, 47(10), 2073–2090. <https://doi.org/10.1111/jbi.13930>
- Alroy, J. (2001). A multispecies overkill simulation of the end-Pleistocene megafaunal mass extinction. *Science*, 292(5523), 1893–1896. <https://doi.org/10.1126/science.1059342>
- Anderson, B. J., Akcakaya, H. R., Araujo, M. B., Fordham, D. A., Martinez-Meyer, E., Thuiller, W., & Brook, B. W. (2009). Dynamics of range margins for metapopulations under climate change. *Proceedings of the Royal Society B: Biological Sciences*, 276(1661), 1415–1420. <https://doi.org/10.1098/rspb.2008.1681>
- Asbjornsen, E. J., Saether, B. E., Linnell, J. D. C., Engen, S., Andersen, R., & Bretten, T. (2005). Predicting the growth of a small introduced muskox population using population prediction intervals. *The Journal of Animal Ecology*, 74(4), 612–618. <https://doi.org/10.1111/j.1365-2656.2005.00946.x>
- Barnosky, A. D., & Lindsey, E. L. (2010). Timing of Quaternary megafaunal extinction in South America in relation to human arrival and climate change. *Quaternary International*, 217(1–2), 10–29. <https://doi.org/10.1016/j.quaint.2009.11.017>
- Bennike, O. (1999). Colonisation of Greenland by plants and animals after the last ice age: A review. *Polar Record*, 35(195), 323–336. <https://doi.org/10.1017/s0032247400015679>
- Berger, J., Hartway, C., Gruzdev, A., & Johnson, M. (2018). Climate degradation and extreme icing events constrain life in cold-adapted mammals. *Scientific Reports*, 8(1), 1156. <https://doi.org/10.1038/s41598-018-19416-9>
- Beumer, L. T., van Beest, F. M., Stelvig, M., & Schmidt, N. M. (2019). Spatiotemporal dynamics in habitat suitability of a large Arctic herbivore: Environmental heterogeneity is key to a sedentary lifestyle. *Global Ecology and Conservation*, 18, e00647. <https://doi.org/10.1016/j.gecco.2019.e00647>
- Beyer, R., Krapp, M., & Manica, A. (2020). An empirical evaluation of bias correction methods for palaeoclimate simulations. *Climate of the Past*, 16(4), 1493–1508. <https://doi.org/10.5194/cp-16-1493-2020>
- Binney, H., Edwards, M., Macias-Fauria, M., Lozhkin, A., Anderson, P., Kaplan, J. O., Andreev, A., Bezrukova, E., Blyakharchuk, T., Jankovska, V., Khazina, I., Krivonogov, S., Kremenetski, K., Nield, J., Novenko, E., Ryabogina, N., Solovieva, N., Willis, K., & Zernitskaya, V. (2017). Vegetation of Eurasia from the last glacial maximum to present: Key biogeographic patterns. *Quaternary Science Reviews*, 157, 80–97. <https://doi.org/10.1016/j.quascirev.2016.11.022>
- Blonder, B., Lamanna, C., Violle, C., & Enquist, B. J. (2014). The n-dimensional hypervolume. *Global Ecology and Biogeography*, 23(5), 595–609. <https://doi.org/10.1111/geb.12146>
- Blonder, B., Morrow, C. B., Maitner, B., Harris, D. J., Lamanna, C., Violle, C., Enquist, B. J., Kerkhoff, A. J., & McMahon, S. (2017). New approaches for delineating n-dimensional hypervolumes. *Methods in Ecology and Evolution*, 9(2), 305–319. <https://doi.org/10.1111/2041-210x.12865>
- Botta, F., Dahl-Jensen, D., Rahbek, C., Svensson, A., & Nogués-Bravo, D. (2019). Abrupt change in climate and biotic systems. *Current Biology*, 29(19), R1045–R1054. <https://doi.org/10.1016/j.cub.2019.08.066>
- Bradshaw, C. J. A., Cooper, A., Turney, C. S. M., & Brook, B. W. (2012). Robust estimates of extinction time in the geological record. *Quaternary Science Reviews*, 33, 14–19. <https://doi.org/10.1016/j.quascirev.2011.11.021>
- Bronk Ramsey, C. (2009). Bayesian analysis of radiocarbon dates. *Radiocarbon*, 51(1), 337–360. <https://doi.org/10.1017/s0033822200033865>
- Brown, J. H., Stevens, G. C., & Kaufman, D. M. (1996). The geographic range: Size, shape, boundaries, and internal structure. *Annual Review of Ecology and Systematics*, 27(1), 597–623. <https://doi.org/10.1146/annurev.ecolsys.27.1.597>

- Brown, S. C., Wigley, T. M. L., Otto-Bliesner, B. L., Rahbek, C., & Fordham, D. A. (2020). Persistent Quaternary climate refugia are hospices for biodiversity in the Anthropocene. *Nature Climate Change*, 10(3), 244–248. <https://doi.org/10.1038/s41558-019-0682-7>
- Campos, P. F., Willerslev, E., Sher, A., Orlando, L., Axelsson, E., Tikhonov, A., Aaris-Sorensen, K., Greenwood, A. D., Kahlke, R. D., Kosintsev, P., Krakhmalnaya, T., Kuznetsova, T., Lemey, P., MacPhee, R., Norris, C. A., Shepherd, K., Suchard, M. A., Zazula, G. D., Shapiro, B., & Gilbert, M. T. (2010). Ancient DNA analyses exclude humans as the driving force behind late Pleistocene musk ox (*Ovibos moschatus*) population dynamics. *Proceedings of the National Academy of Sciences of the United States of America*, 107(12), 5675–5680. <https://doi.org/10.1073/pnas.0907189107>
- Canteri, E., Brown, S. C., Schmidt, N. M., Heller, R., Nogues-Bravo, D., & Fordham, D. A. (2022). Data from: Spatiotemporal influences of climate and humans on muskox range dynamics over multiple millennia. *Dryad Digital Repository*, <https://doi.org/10.5061/dryad.3r2280gjj>
- Chevalier, M., Davis, B. A. S., Heiri, O., Seppä, H., Chase, B. M., Gajewski, K., Lacourse, T., Telford, R. J., Finsinger, W., Guiot, J., Kühl, N., Maezumi, S. Y., Tipton, J. R., Carter, V. A., Brussel, T., Phelps, L. N., Dawson, A., Zanon, M., Vallé, F., ... Kupriyanov, D. (2020). Pollen-based climate reconstruction techniques for late Quaternary studies. *Earth-Science Reviews*, 210, 103384. <https://doi.org/10.1016/j.earscirev.2020.103384>
- Clark, P. U., Shakun, J. D., Baker, P. A., Bartlein, P. J., Brewer, S., Brook, E., Carlson, A. E., Cheng, H., Kaufman, D. S., Liu, Z., Marchitto, T. M., Mix, A. C., Morrill, C., Otto-Bliesner, B. L., Pahnke, K., Russell, J. M., Whitlock, C., Adkins, J. F., Blois, J. L., ... Williams, J. W. (2012). Global climate evolution during the last deglaciation. *Proceedings of the National Academy of Sciences of the United States of America*, 109(19), E1134–E1142. <https://doi.org/10.1073/pnas.1116619109>
- Connolly, S. R., Keith, S. A., Colwell, R. K., & Rahbek, C. (2017). Process, mechanism, and modeling in macroecology. *Trends in Ecology & Evolution*, 32(11), 835–844. <https://doi.org/10.1016/j.tree.2017.08.011>
- Cooper, A., Turney, C., Hughen, K. A., Brook, B. W., McDonald, H. G., & Bradshaw, C. J. (2015). Abrupt warming events drove Late Pleistocene Holarctic megafaunal turnover. *Science*, 349(6248), 602–606. <https://doi.org/10.1126/science.aac4315>
- Csilléry, K., Blum, M. G., Gaggiotti, O. E., & Francois, O. (2010). Approximate Bayesian Computation (ABC) in practice. *Trends in Ecology & Evolution*, 25(7), 410–418. <https://doi.org/10.1016/j.tree.2010.04.001>
- Csilléry, K., François, O., & Blum, M. G. B. (2012). abc: An R package for Approximate Bayesian Computation (ABC). *Methods in Ecology and Evolution*, 3(3), 475–479. <https://doi.org/10.1111/j.2041-210X.2011.00179.x>
- Cuyler, C., Rowell, J., Adamczewski, J., Anderson, M., Blake, J., Bretten, T., Brodeur, V., Campbell, M., Checkley, S. L., Cluff, H. D., Côté, S. D., Davison, T., Dumond, M., Ford, B., Gruzdev, A., Gunn, A., Jones, P., Kutz, S., Leclerc, L. M., ... Ytrehus, B. (2020). Muskox status, recent variation, and uncertain future. *Ambio*, 49, 805–819. <https://doi.org/10.1007/s13280-019-01205-x>
- Dansgaard, W., Johnsen, S. J., Clausen, H. B., Dahl-Jensen, D., Gundestrup, N. S., Hammer, C. U., Hvidberg, C. S., Steffensen, J. P., Sveinbjörnsdóttir, A. E., Jouzel, J., & Bond, G. (1993). Evidence for general instability of past climate from a 250-kyr ice-core record. *Nature*, 364(6434), 218–220. <https://doi.org/10.1038/364218a0>
- Desforges, J. P., Marques, G. M., Beumer, L. T., Chimienti, M., Hansen, L. H., Pedersen, S. H., Schmidt, N. M., & van Beest, F. M. (2021). Environment and physiology shape Arctic ungulate population dynamics. *Global Change Biology*, 27(9), 1755–1771. <https://doi.org/10.1111/gcb.15484>
- Dolédéc, S., Chessel, D., & Gimaret-Carpentier, C. (2000). Niche separation in community analysis: A new method. *Ecology*, 81(10), 2914–2927. [https://doi.org/10.1890/0012-9658\(2000\)081\[2914:Nsicaa\]2.0.Co;2](https://doi.org/10.1890/0012-9658(2000)081[2914:Nsicaa]2.0.Co;2)
- Dormann, C. F., Elith, J., Bacher, S., Buchmann, C., Carl, G., Carré, G., Marquéz, J. R. G., Gruber, B., Lafourcade, B., Leitão, P. J., Münkemüller, T., McClean, C., Osborne, P. E., Reineking, B., Schröder, B., Skidmore, A. K., Zurell, D., & Lautenbach, S. (2013). Collinearity: A review of methods to deal with it and a simulation study evaluating their performance. *Ecography*, 36(1), 27–46. <https://doi.org/10.1111/j.1600-0587.2012.07348.x>
- Eriksson, A., Betti, L., Friend, A. D., Lycett, S. J., Singarayer, J. S., von Cramon-Taubadel, N., Valdes, P. J., Balloux, F., & Manica, A. (2012). Late Pleistocene climate change and the global expansion of anatomically modern humans. *Proceedings of the National Academy of Sciences of the United States of America*, 109(40), 16089–16094. <https://doi.org/10.1073/pnas.1209494109>
- Fordham, D. A., Akçakaya, H. R., Alroy, J., Saltré, F., Wigley, T. M. L., & Brook, B. W. (2016). Predicting and mitigating future biodiversity loss using long-term ecological proxies. *Nature Climate Change*, 6(10), 909–916. <https://doi.org/10.1038/nclimate3086>
- Fordham, D. A., Akçakaya, H. R., Brook, B. W., Rodríguez, A., Alves, P. C., Civantos, E., Triviño, M., Watts, M. J., & Araújo, M. B. (2013). Adapted conservation measures are required to save the Iberian lynx in a changing climate. *Nature Climate Change*, 3(10), 899–903. <https://doi.org/10.1038/nclimate1954>
- Fordham, D. A., Bertelsmeier, C., Brook, B. W., Early, R., Neto, D., Brown, S. C., Ollier, S., & Araujo, M. B. (2018). How complex should models be? Comparing correlative and mechanistic range dynamics models. *Global Change Biology*, 24(3), 1357–1370. <https://doi.org/10.1111/gcb.13935>
- Fordham, D. A., Brook, B. W., Moritz, C., & Nogues-Bravo, D. (2014). Better forecasts of range dynamics using genetic data. *Trends in Ecology & Evolution*, 29(8), 436–443. <https://doi.org/10.1016/j.tree.2014.05.007>
- Fordham, D. A., Brown, S. C., Akçakaya, H. R., Brook, B. W., Haythorne, S., Manica, A., Shoemaker, K. T., Austin, J. J., Blonder, B., Pilowsky, J., Rahbek, C., & Nogues-Bravo, D. (2022). Process-explicit models reveal pathway to extinction for woolly mammoth using pattern-oriented validation. *Ecology Letters*, 25(1), 125–137. <https://doi.org/10.1111/ele.13911>
- Fordham, D. A., Haythorne, S., Brown, S. C., Buettel, J. C., & Brook, B. W. (2021). poems: R package for simulating species' range dynamics using pattern-oriented validation. *Methods in Ecology and Evolution*, 12(12), 2364–2371. <https://doi.org/10.1111/2041-210X.13720>
- Fordham, D. A., Jackson, S. T., Brown, S. C., Huntley, B., Brook, B. W., Dahl-Jensen, D., Gilbert, M. T. P., Otto-Bliesner, B. L., Svensson, A., Theodoridis, S., Wilmshurst, J. M., Buettel, J. C., Canteri, E., McDowell, M., Orlando, L., Pilowsky, J., Rahbek, C., & Nogues-Bravo, D. (2020). Using paleo-archives to safeguard biodiversity under climate change. *Science*, 369(6507), 10. <https://doi.org/10.1126/science.abc5654>
- Fordham, D. A., Saltré, F., Haythorne, S., Wigley, T. M. L., Otto-Bliesner, B. L., Chan, K. C., & Brook, B. W. (2017). PaleoView: A tool for generating continuous climate projections spanning the last 21000 years at regional and global scales. *Ecography*, 40(11), 1348–1358. <https://doi.org/10.1111/ecog.03031>
- Fordham, D. A., Wigley, T. M. L., & Brook, B. W. (2011). Multi-model climate projections for biodiversity risk assessments. *Ecological Applications*, 21(8), 3317–3331. <https://doi.org/10.1890/11-0314.1>
- Foster, J., Liston, G., Koster, R., Essery, R., Behr, H., Dumenil, L., Versegny, D., Thompson, S., Pollard, D., & Cohen, J. (1996). Snow cover and snow mass intercomparisons of general circulation models and remotely sensed datasets. *Journal of Climate*, 9(2), 409–426. [https://doi.org/10.1175/1520-0442\(1996\)009<0409:scasmi>2.0.co;2](https://doi.org/10.1175/1520-0442(1996)009<0409:scasmi>2.0.co;2)
- Gaston, K. J. (2003). *The structure and dynamics of geographic ranges*. Oxford University Press.
- GBIF.org. (2019). *GBIF occurrence download [Occurrence data]*. The Global Biodiversity Information Facility.

- Grimm, V., & Railsback, S. F. (2012). Pattern-oriented modelling: A 'multi-scope' for predictive systems ecology. *Philosophical Transactions of the Royal Society of London. Series B, Biological Sciences*, 367(1586), 298–310. <https://doi.org/10.1098/rstb.2011.0180>
- Grimm, V., Revilla, E., Berger, U., Jeltsch, F., Mooij, W. M., Railsback, S. F., Thulke, H. H., Weiner, J., Wiegand, T., & DeAngelis, D. L. (2005). Pattern-oriented modeling of agent-based complex systems: Lessons from ecology. *Science*, 310(5750), 987–991. <https://doi.org/10.1126/science.1116681>
- Hagen, O., Fluck, B., Fopp, F., Cabral, J. S., Hartig, F., Pontarp, M., Rangel, T. F., & Pellissier, L. (2021). gen3sis: A general engine for eco-evolutionary simulations of the processes that shape Earth's biodiversity. *PLoS Biology*, 19(7), e3001340. <https://doi.org/10.1371/journal.pbio.3001340>
- Haile, J., Froese, D. G., Macphee, R. D., Roberts, R. G., Arnold, L. J., Reyes, A. V., Rasmussen, M., Nielsen, R., Brook, B. W., Robinson, S., Demuro, M., Gilbert, M. T., Munch, K., Austin, J. J., Cooper, A., Barnes, I., Moller, P., & Willerslev, E. (2009). Ancient DNA reveals late survival of mammoth and horse in interior Alaska. *Proceedings of the National Academy of Sciences of the United States of America*, 106(52), 22352–22357. <https://doi.org/10.1073/pnas.0912510106>
- Hansen, C. C. R., Hvilsum, C., Schmidt, N. M., Aastrup, P., Van Coeverden de Groot, P. J., Siegismund, H. R., & Heller, R. (2018). The muskox lost a substantial part of its genetic diversity on its long road to Greenland. *Current Biology*, 28(24), 4022–4028.e4025. <https://doi.org/10.1016/j.cub.2018.10.054>
- Harris, I., Osborn, T. J., Jones, P., & Lister, D. (2020). Version 4 of the CRU TS monthly high-resolution gridded multivariate climate dataset. *Scientific Data*, 7(1), 109. <https://doi.org/10.1038/s41597-020-0453-3>
- Haythorne, S., Fordham, D., Brown, S., Buettel, J., & Brook, B. (2021). *poems: Pattern-oriented ensemble modeling system*. (version 1.0.1) [R package]. R. <https://CRAN.R-project.org/package=poems>
- Haythorne, S., Pilowsky, J., Brown, S., & Fordham, D. (2021). *paleopop: Pattern-oriented modeling framework for coupled niche-population paleo-climatic models*. (version 2.1.2) [R package]. R. <https://CRAN.R-project.org/package=paleopop>
- Heard, D. C. (1992). The effect of wolf predation and snow cover on musk-ox group size. *The American Naturalist*, 139(1), 190–204. <http://www.jstor.org.proxy.library.adelaide.edu.au/stable/2462592>
- Kafle, P., Peller, P., Massolo, A., Hoberg, E., Leclerc, L. M., Tomaselli, M., & Kutz, S. (2020). Range expansion of muskox lungworms track rapid arctic warming: Implications for geographic colonization under climate forcing. *Scientific Reports*, 10(1), 17323. <https://doi.org/10.1038/s41598-020-74358-5>
- Kaufman, D. (2004). Holocene thermal maximum in the western Arctic (0–180°W). *Quaternary Science Reviews*, 23(5–6), 529–560. <https://doi.org/10.1016/j.quascirev.2003.09.007>
- Kristensen, D. K., Kristensen, E., Forchhammer, M. C., Michelsen, A., & Schmidt, N. M. (2011). Arctic herbivore diet can be inferred from stable carbon and nitrogen isotopes in C3 plants, faeces, and wool. *Canadian Journal of Zoology*, 89(10), 892–899. <https://doi.org/10.1139/z11-073>
- Lee, J.-Y., Marotzke, J., Bala, G., Cao, L., Corti, S., Dunne, J. P., Engelbrecht, F., Fischer, E., Fyfe, J. C., Jones, C., Maycock, A., Mutemi, J., Ndiaye, O., Panickal, S., & Zhou, T. (2021). Future global climate: Scenario-based projections and near-term information. In V. Masson-Delmotte, P. Zhai, A. Pirani, S. L. Connors, C. Péan, S. Berger, N. Caud, Y. Chen, L. Goldfarb, M. I. Gomis, M. Huang, K. Leitzell, E. Lonnoy, J. B. R. Matthews, T. K. Maycock, T. Waterfield, O. Yelekçi, R. Yu, & B. Zhou (Eds.), *Climate change 2021: The physical science basis. Contribution of Working Group I to the Sixth Assessment Report of the Intergovernmental Panel on Climate Change*. Cambridge University Press.
- Lent, P. C. (1999). *Muskoxen and their hunters: A history* (Vol. 5). University of Oklahoma Press.
- Lister, A. M., & Stuart, A. J. (2008). The impact of climate change on large mammal distribution and extinction: Evidence from the last glacial/interglacial transition. *Comptes Rendus Geosciences*, 340(9–10), 615–620. <https://doi.org/10.1016/j.crte.2008.04.001>
- Liu, A. Z., Otto-Bliesner, A. B. L., He, A. F., Brady, A. E. C., Tomas, A. R., Clark, A. P. U., Carlson, A. A. E., Lynch-Stieglitz, A. J., Curry, A. W., Brook, A. E., Erickson, A. D., Jacob, A. R., Kutzbach, A. J., & Cheng, A. J. (2009). Transient simulation of last deglaciation with a new mechanism for Bølling-Allerød warming. *Science*, 325(5938), 310–314. <https://doi.org/10.1126/science.1171041>
- Lord, E., Dussex, N., Kierczak, M., Diez-Del-Molino, D., Ryder, O. A., Stanton, D. W. G., Gilbert, M. T. P., Sanchez-Barreiro, F., Zhang, G., Sinding, M. S., Lorenzen, E. D., Willerslev, E., Protopopov, A., Shidlovskiy, F., Fedorov, S., Bocherens, H., Nathan, S., Goossens, B., van der Plicht, J., ... Dalen, L. (2020). Pre-extinction demographic stability and genomic signatures of adaptation in the Woolly Rhinoceros. *Current Biology*, 30(19), 3871–3879.e3877. <https://doi.org/10.1016/j.cub.2020.07.046>
- Lorenzen, E. D., Nogués-Bravo, D., Orlando, L., Weinstock, J., Binladen, J., Marske, K. A., Ugan, A., Borregaard, M. K., Gilbert, M. T., Nielsen, R., Ho, S. Y., Goebel, T., Graf, K. E., Byers, D., Stenderup, J. T., Rasmussen, M., Campos, P. F., Leonard, J. A., Koepfli, K. P., ... Willerslev, E. (2011). Species-specific responses of Late Quaternary megafauna to climate and humans. *Nature*, 479(7373), 359–364. <https://doi.org/10.1038/nature10574>
- Mann, D. H., Groves, P., Kunz, M. L., Reanier, R. E., & Gaglioti, B. V. (2013). Ice-age megafauna in Arctic Alaska: Extinction, invasion, survival. *Quaternary Science Reviews*, 70, 91–108. <https://doi.org/10.1016/j.quascirev.2013.03.015>
- Markova, A. K., Puzachenko, A. Y., van Kolfschoten, T., Kosintsev, P. A., Kuznetsova, T. V., Tikhonov, A. N., Bachura, O. P., Ponomarev, D. V., van der Plicht, J., & Kuitens, M. (2015). Changes in the Eurasian distribution of the musk ox (*Ovibos moschatus*) and the extinct bison (*Bison priscus*) during the last 50 ka BP. *Quaternary International*, 378, 99–110. <https://doi.org/10.1016/j.quaint.2015.01.020>
- McCarthy, M. A., & Thompson, C. (2001). Expected minimum population size as a measure of threat. *Animal Conservation*, 4(4), 351–355. <https://doi.org/10.1017/s136794300100141x>
- McKay, M. D., Beckman, R. J., & Conover, W. J. (1979). A comparison of three methods for selecting values of input variables in the analysis of output from a computer code. *Technometrics*, 21(2), 239–245. <https://doi.org/10.2307/1268522>
- Meldgaard, M. (1986). *The Greenland Caribou-zoogeography, taxonomy and population dynamics* (Bioscience Ed., Vol. 20). The Commission for Scientific Research in Greenland.
- Meredith, M., Sommerkorn, M., Cassotta, S., Derksen, C., Ekaykin, A., Hollowed, A., Kofinas, G., Mackintosh, A., Melbourne-Thomas, J., Muelbert, M. M. C., Ottersen, G., Pritchard, H., & Schuur, E. A. G. (2019). Polar regions. In H.-O. Pörtner, D. C. Roberts, V. Masson-Delmotte, P. Zhai, M. Tignor, E. Poloczanska, & N. Weyer (Eds.), *IPCC Special Report on the Ocean and Cryosphere in a Changing Climate*. Intergovernmental Panel on Climate Change.
- Murchie, T. J., Monteath, A. J., Mahony, M. E., Long, G. S., Cocker, S., Sadoway, T., Karpinski, E., Zazula, G., MacPhee, R. D. E., Froese, D., & Poinar, H. N. (2021). Collapse of the mammoth-steppe in central Yukon as revealed by ancient environmental DNA. *Nature Communications*, 12(1), 7120. <https://doi.org/10.1038/s41467-021-27439-6>
- Nogués-Bravo, D. (2009). Predicting the past distribution of species climatic niches. *Global Ecology and Biogeography*, 18(5), 521–531. <https://doi.org/10.1111/j.1466-8238.2009.00476.x>
- Nogués-Bravo, D., Ohlemüller, R., Batra, P., & Araujo, M. B. (2010). Climate predictors of late quaternary extinctions. *Evolution*, 64(8), 2442–2449. <https://doi.org/10.1111/j.1558-5646.2010.01009.x>

- Nogues-Bravo, D., Rodriguez-Sanchez, F., Orsini, L., de Boer, E., Jansson, R., Morlon, H., Fordham, D. A., & Jackson, S. T. (2018). Cracking the code of biodiversity responses to past climate change. *Trends in Ecology & Evolution*, 33(10), 765–776. <https://doi.org/10.1016/j.tree.2018.07.005>
- Orlando, L., & Cooper, A. (2014). Using ancient DNA to understand evolutionary and ecological processes. *Annual Review of Ecology, Evolution, and Systematics*, 45(1), 573–598. <https://doi.org/10.1146/annurev-ecolsys-120213-091712>
- Pilowsky, J. A., Colwell, R. K., Rahbek, C., & Fordham, D. A. (2022). Process-explicit models reveal the structure and dynamics of biodiversity. *Science Advances*, 8, eabj2271. <https://doi.org/10.1126/sciadv.abj2271>
- Post, E. (2013). Erosion of community diversity and stability by herbivore removal under warming. *Proceedings of the Royal Society B: Biological Sciences*, 280(1757), 20122722. <https://doi.org/10.1098/rspb.2012.2722>
- Post, E., Alley, R. B., Christensen, T. R., Macias-Fauria, M., Forbes, B. C., Gooseff, M. N., Iler, A., Kerby, J. T., Laidre, K. L., Mann, M. E., Olofsson, J., Stroeve, J. C., Ulmer, F., Virginia, R. A., & Wang, M. (2019). The polar regions in a 2°C warmer world. *Science Advances*, 5(12), eaaw9883. <https://doi.org/10.1126/sciadv.aaw9883>
- Post, E., & Pedersen, C. (2008). Opposing plant community responses to warming with and without herbivores. *Proceedings of the National Academy of Sciences of the United States of America*, 105(34), 12353–12358. <https://doi.org/10.1073/pnas.0802421105>
- Prowse, T. A. A., Bradshaw, C. J. A., Delean, S., Cassey, P., Lacy, R. C., Wells, K., Aiello-Lammens, M. E., Akçakaya, H. R., & Brook, B. W. (2016). An efficient protocol for the global sensitivity analysis of stochastic ecological models. *Ecosphere*, 7(3), e01238. <https://doi.org/10.1002/ecs2.1238>
- Raghavan, M., Steinrücken, M., Harris, K., Schiffels, S., Rasmussen, S., Degiorgio, M., Albrechtsen, A., Valdiosera, C., Ávila-Arcos, M. C., Malaspina, A.-S., Eriksson, A., Moltke, I., Metspalu, M., Homburger, J. R., Wall, J., Cornejo, O. E., Moreno-Mayar, J. V., Korneliusson, T. S., Pierre, T., ... Willerslev, E. (2015). Genomic evidence for the Pleistocene and recent population history of Native Americans. *Science*, 349(6250), aab3884. <https://doi.org/10.1126/science.aab3884>
- Rangel, T. F., Edwards, N. R., Holden, P. B., Diniz-Filho, J. A. F., Gosling, W. D., Coelho, M. T. P., Cassemiro, F. A. S., Rahbek, C., & Colwell, R. K. (2018). Modeling the ecology and evolution of biodiversity: Biogeographical cradles, museums, and graves. *Science*, 361(6399), eaar5452. <https://doi.org/10.1126/science.aar5452>
- Reimer, P. J., Austin, W. E. N., Bard, E., Bayliss, A., Blackwell, P. G., Bronk Ramsey, C., Butzin, M., Cheng, H., Edwards, R. L., Friedrich, M., Grootes, P. M., Guilderson, T. P., Hajdas, I., Heaton, T. J., Hogg, A. G., Hughen, K. A., Kromer, B., Manning, S. W., Muscheler, R., ... Talamo, S. (2020). The IntCal20 Northern Hemisphere radiocarbon age calibration curve (0–55 cal kBP). *Radiocarbon*, 62(4), 725–757. <https://doi.org/10.1017/rdc.2020.41>
- Reynolds, P. E., Reynolds, H. V., & Shideler, R. T. (2002). Predation and multiple kills of muskoxen by grizzly bears. *Ursus*, 13, 79–84. <https://www.jstor.org/stable/3873189>
- Ricker, W. E. (1954). Stock and recruitment. *Journal of the Fisheries Research Board of Canada*, 11(5), 559–623.
- Schmidt, N. M., Mosbacher, J. B., Vesterinen, E. J., Roslin, T., & Michelsen, A. (2018). Limited dietary overlap amongst resident Arctic herbivores in winter: Complementary insights from complementary methods. *Oecologia*, 187(3), 689–699. <https://doi.org/10.1007/s00442-018-4147-x>
- Schmidt, N. M., van Beest, F. M., Mosbacher, J. B., Stelvig, M., Hansen, L. H., Nabe-Nielsen, J., & Grondahl, C. (2016). Ungulate movement in an extreme seasonal environment: Year-round movement patterns of high-arctic muskoxen. *Wildlife Biology*, 22(6), 253–267. <https://doi.org/10.2981/wlb.00219>
- Screen, J. A., & Simmonds, I. (2010). The central role of diminishing sea ice in recent Arctic temperature amplification. *Nature*, 464(7293), 1334–1337. <https://doi.org/10.1038/nature09051>
- Smith, C. I., Chamberlain, A. T., Riley, M. S., Stringer, C., & Collins, M. J. (2003). The thermal history of human fossils and the likelihood of successful DNA amplification. *Journal of Human Evolution*, 45(3), 203–217. [https://doi.org/10.1016/s0047-2484\(03\)00106-4](https://doi.org/10.1016/s0047-2484(03)00106-4)
- Steffensen, J. P., Andersen, K. K., Bigler, M., Clausen, H. B., Dahl-Jensen, D., Fischer, H., Goto-Azuma, K., Hansson, M., Johnsen, S. J., Jouzel, J., Masson-Delmotte, V., Popp, T., Rasmussen, S. O., Rothlisberger, R., Ruth, U., Stauffer, B., Siggaard-Andersen, M.-L., Sveinbjornsdottir, A. E., Svensson, A., & White, J. W. C. (2008). High-resolution Greenland ice core data show abrupt climate change happens in few years. *Science*, 321(5889), 680–684. <https://doi.org/10.1126/science.1157707>
- Stephens, L., Fuller, D., Boivin, N., Rick, T., Gauthier, N., Kay, A., Marwick, B., Armstrong, C. G., Barton, C. M., Denham, T., Douglass, K., Driver, J., Janz, L., Roberts, P., Rogers, J. D., Thakar, H., Altaweel, M., Johnson, A. L., Sampietro Vattuone, M. M., ... Ellis, E. (2019). Archaeological assessment reveals Earth's early transformation through land use. *Science*, 365(6456), 897–902. <https://doi.org/10.1126/science.aax1192>
- Strobl, C., Boulesteix, A. L., Zeileis, A., & Hothorn, T. (2007). Bias in random forest variable importance measures: Illustrations, sources and a solution. *BMC Bioinformatics*, 8(1), 25. <https://doi.org/10.1186/1471-2105-8-25>
- Stuart, A. J. (2015). Late Quaternary megafaunal extinctions on the continents: A short review. *Geological Journal*, 50(3), 338–363. <https://doi.org/10.1002/gj.2633>
- Stuart, A. J., & Lister, A. M. (2011). Extinction chronology of the cave lion *Panthera spelaea*. *Quaternary Science Reviews*, 30(17–18), 2329–2340. <https://doi.org/10.1016/j.quascirev.2010.04.023>
- Stuart, A. J., & Lister, A. M. (2012). Extinction chronology of the woolly rhinoceros *Coelodonta antiquitatis* in the context of late Quaternary megafaunal extinctions in northern Eurasia. *Quaternary Science Reviews*, 51, 1–17. <https://doi.org/10.1016/j.quascirev.2012.06.007>
- Svenning, J.-C., Fløjgaard, C., Marske, K. A., Nógues-Bravo, D., & Normand, S. (2011). Applications of species distribution modeling to paleobiology. *Quaternary Science Reviews*, 30(21–22), 2930–2947. <https://doi.org/10.1016/j.quascirev.2011.06.012>
- van Beest, F. M., Beumer, L. T., Andersen, A. S., Hansson, S. V., Schmidt, N. M., & Zhang, Z. (2021). Rapid shifts in Arctic tundra species' distributions and inter-specific range overlap under future climate change. *Diversity and Distributions*, 27(9), 1706–1718. <https://doi.org/10.1111/ddi.13362>
- van der Vaart, E., Beaumont, M. A., Johnston, A. S. A., & Sibly, R. M. (2015). Calibration and evaluation of individual-based models using Approximate Bayesian Computation. *Ecological Modelling*, 312, 182–190. <https://doi.org/10.1016/j.ecolmodel.2015.05.020>
- Wang, Y., Pedersen, M. W., Alsos, I. G., De Sanctis, B., Racimo, F., Prohaska, A., Coissac, E., Owens, H. L., Merkel, M. K. F., Fernandez-Guerra, A., Rouillard, A., Lammers, Y., Alberti, A., Denoeud, F., Money, D., Ruter, A. H., Mccoll, H., Larsen, N. K., Cherezova, A. A., ... Willerslev, E. (2021). Late Quaternary dynamics of Arctic biota from ancient environmental genomics. *Nature*, 600, 86–92. <https://doi.org/10.1038/s41586-021-04016-x>
- Wanner, H., Beer, J., Bütikofer, J., Crowley, T. J., Cubasch, U., Flückiger, J., Goosse, H., Grosjean, M., Joos, F., Kaplan, J. O., Küttel, M., Müller, S. A., Prentice, I. C., Solomina, O., Stocker, T. F., Tarasov, P., Wagner, M., & Widmann, M. (2008). Mid- to Late Holocene climate change: An overview. *Quaternary Science Reviews*, 27(19–20), 1791–1828. <https://doi.org/10.1016/j.quascirev.2008.06.013>
- Willerslev, E., Hansen, A. J., Binladen, J., Brand, T. B., Gilbert, M. T. P., Shapiro, B., Bunce, M., Wiuf, C., Gilichinsky, D. A., & Cooper, A. (2003). Diverse plant and animal genetic records from Holocene and Pleistocene sediments. *Science*, 300(5620), 791–795. <https://doi.org/10.1126/science.1084114>

- Wright, M. N., & Ziegler, A. (2017). ranger: A fast implementation of random forests for high dimensional data in C++ and R [C++; classification; machine learning; R; random forests; Rcpp; recursive partitioning; survival analysis]. *Journal of Statistical Software*, 77(1), 17. <https://doi.org/10.18637/jss.v077.i01>
- Yannic, G., Hagen, O., Leugger, F., Karger, D. N., & Pellissier, L. (2020). Harnessing paleo-environmental modeling and genetic data to predict intraspecific genetic structure. *Evolutionary Applications*, 13(6), 1526–1542. <https://doi.org/10.1111/eva.12986>
- Yannic, G., Pellissier, L., Ortego, J., Lecomte, N., Couturier, S., Cuyler, C., Dussault, C., Hundertmark, K. J., Irvine, R. J., Jenkins, D. A., Kolpashikov, L., Mager, K., Musiani, M., Parker, K. L., Roed, K. H., Sipko, T., Porisson, S. G., Weckworth, B. V., Guisan, A., ... Cote, S. D. (2014). Genetic diversity in caribou linked to past and future climate change. *Nature Climate Change*, 4(2), 132–137. <https://doi.org/10.1038/Nclimate2074>
- Zimov, S. A., Chuprynin, V. I., Oreshko, A. P., Chapin, F. S., Reynolds, J. F., & Chapin, M. C. (1995). Steppe-tundra transition: A herbivore-driven

biome shift at the end of the pleistocene. *The American Naturalist*, 146(5), 765–794. <https://doi.org/10.1086/285824>

#### SUPPORTING INFORMATION

Additional supporting information can be found online in the Supporting Information section at the end of this article.

**How to cite this article:** Canteri, E., Brown, S. C., Schmidt, N. M., Heller, R., Nogués-Bravo, D., & Fordham, D. A. (2022). Spatiotemporal influences of climate and humans on muskox range dynamics over multiple millennia. *Global Change Biology*, 28, 6602–6617. <https://doi.org/10.1111/gcb.16375>